SUPPORTING INFORMATION for

Boundary Conditions for Diffusion-Mediated Processes within Linear Nanopores: Exact Treatment of Coupling to an Equilibrated External Fluid

Andrés García and James W. Evans

Division of Chemical and Biological Sciences, Ames Laboratory – USDOE and Department of Physics & Astronomy, Iowa State University, Ames, Iowa 50011

Journal of Physical Chemistry C (2017).

S1. BOUNDARY CONDITIONS FOR A *1X1XL* CELL PORE WITH $R = 2$

To illustrate the additional complications in treating models with longer interaction range $R \geq 2$, we consider the simplest case: the *1x1xL* cell model for $R = 2$, i.e., no pairs of particles with separations 2 or less. In this case, there are no pairs of particles in the 3D fluid with separations 1, $\sqrt{2}$, $\sqrt{3}$, or 2. The maximum concentration in this model is $\langle X_{max} \rangle = 1/3$ within the pore. The rate of adsorption to an end site within the pore is given by

$$R_{ads} = h\langle C_{0,0,0}\, E_1\, E_2\, E_3 \rangle = h\langle C_{0,0,0} | E_1\, E_2\, E_3 \rangle \langle E_1\, E_2\, E_3 \rangle = h\langle C_0 \rangle \langle E_1\, E_2\, E_3 \rangle. \qquad \text{(S1.1)}$$

Using the spatial Markov property that a pair of cells shields for $R = 2$, one has $\langle C_0 \rangle = \langle C_{0,0,0} | E_1\, E_2\, E_3 \rangle = \langle C_{0,0,0} | E_1\, E_2 \rangle$ is the conditional concentration, $\langle C_0 \rangle$, at cells just outside the pore opening given that the end pair of sites within the pore are empty. Again, $\langle C_0 \rangle$ corresponds to the concentration in the layer against the wall for a semi-infinite system, and can be determined from a *tailored simulation*. See Figure S1a.

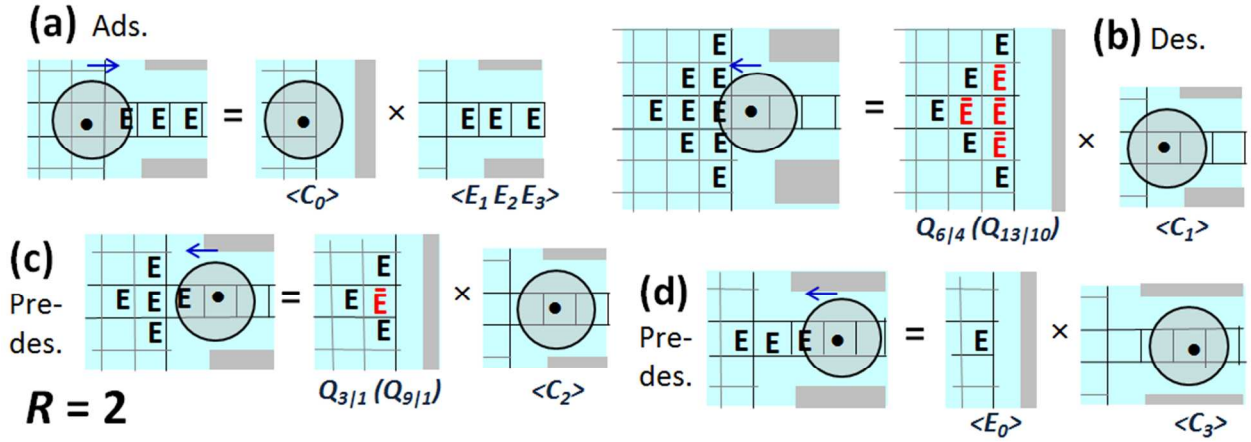

Figure S1. 2D schematic of configurations relevant for adsorption, desorption, and pre-desorption in *1x1xL* cell model for $R = 2$. E denotes empty cells; Ē in red text denotes cells prescribed to be empty. Conditional probabilities, $Q_{n|m}$, indicating the number of sites required (n) and given (m) empty for a 2D (3D) exterior fluid lattice.

Desorption from an end site within the pore to the exterior fluid requires 23 sites just outside the pore to be empty in 3D. Using the spatial Markov property, the associated rate of desorption is given by

$$R_{des} = h\, Q_{13|10} \langle C_1 \rangle. \qquad \text{(S1.2)}$$

Here, $Q_{13|10}$ is the conditional probability for 13 cells to be empty given 10 cells closest to the pore opening are empty in 3D. $Q_{13|10}$ is determined from a *second tailored simulation* for a semi-infinite system with 10 cell against the wall specified empty. See Figure S1b.

Stand-alone simulations must also treat the pre-desorption step of hopping from cell 2 to cell 1 at the end of the pore which requires 10 cells just outside the pore to be empty in 3D. Analysis of the associated conditional probability, $Q_{9|1}$, requires a *third tailored simulation* given one cell against the wall in a semi-infinite system is specified empty. See Figure S1c. One must also treat hopping from cell 3 to cell 2 which requires a single cell just outside the opening of the pore to be empty. See again Figure S1d.

S2. MEAN-FIELD TYPE TREATMENTS OF TRACER DIFFUSIVITY

Below, $J_C^{k>k+1}$ denotes the net flux of C = A or B from cell layer k to k+1. We consider behavior in a counter diffusion mode where the pore is occupied by just A and B such that the total concentration of particles X = A + B or either type is constant (at least in the pore interior). Thus $\langle X_{int} \rangle$ and $\langle E_{int} \rangle = 1 - \langle X_{int} \rangle$ are independent of k. Schematics of the multi-cell probabilities associated with this diffusion flux are given in Figure S2 for the *1x1xL* cell model with $R = 0$, the *2x1xL* cell model with $R = 1$, and the *2x2xL* cell model with $R = \sqrt{2}$.

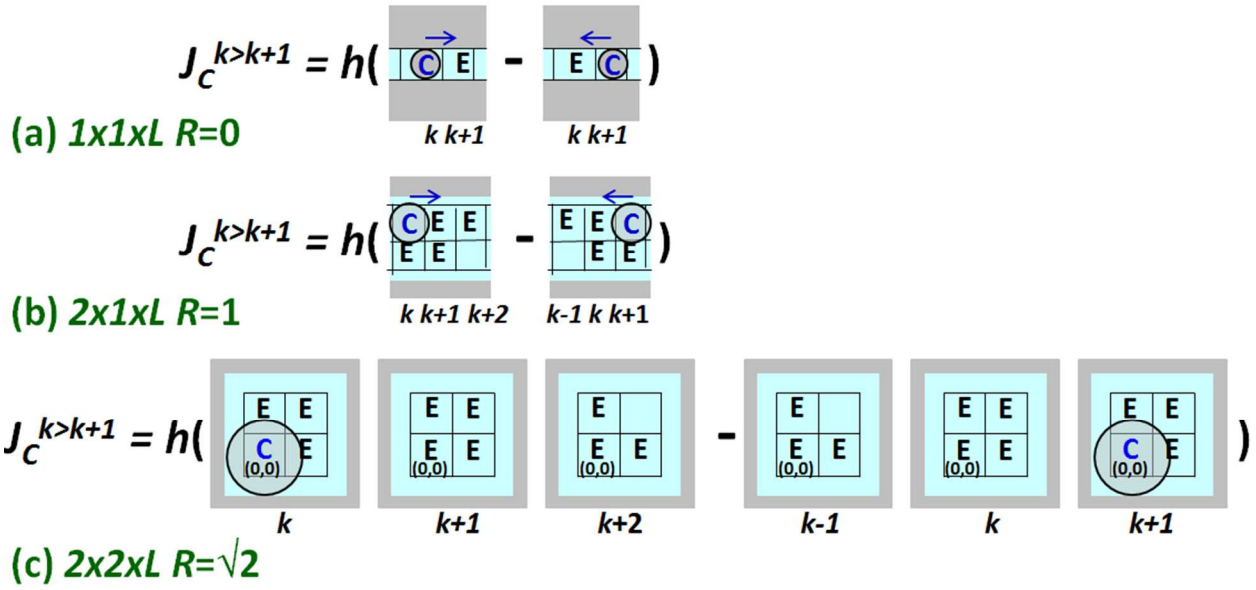

Figure S2. Schematic of multi-cell configurations probabilities defining $J_C^{k>k+1}$ for the: (a) *1x1xL* cell model with $R = 0$; (b) *2x1xL* cell model with $R = 1$; and (c) *2x2xL* cell model with $R = \sqrt{2}$.

First, we consider behavior for the *1x1xL* cell model with $R = 0$ where it is natural to apply a standard mean-field (MF) site approximation to obtain (cf. Figure S2a)

$$J_C^{k>k+1} = h\,(\langle C_k E_{k+1}\rangle - \langle E_k C_{k+1}\rangle)$$

$$\approx h\,(\langle C_k\rangle\langle E_{k+1}\rangle - \langle E_k\rangle\langle C_{k+1}\rangle) = -h\langle E_{int}\rangle\ \nabla\langle C_{k+1}\rangle. \qquad \text{(S2.1)}$$

where $\nabla\langle C_k\rangle = \langle C_k\rangle - \langle C_{k+1}\rangle$. We thus conclude that

$$D_{tr}(1x1xL,\ R=0,\ MF \text{ site}) = h\langle E_{int}\rangle = h(1-\langle X_{int}\rangle). \qquad \text{(S2.2)}$$

This result implies that $D_{tr}(1x1xL,\ R=0,\ MF$ site$) = 0.6h$ for $\langle X_{int}\rangle = 0.4$ which is significantly above $D_{tr}(\max) \approx 0.32h$ for this model with $L \geq 25$.

For any model with $R > 0$, the site approximation is inadequate as it does not account for the exclusion of nearby pairs of particles. However, the pair approximation is reasonable for the *2x1xL* cell model with NN exclusion. We now consider the *2x2xL* cell model with $R = 1$. Here, we use the simplified notation $\langle C_{0,j,k}\rangle = \langle C_{j,k}\rangle$ for cells within the pore where $j = 0$ or 1 and $1 \leq k \leq L$. After applying the standard pair approximation to factorize the probabilities of multi-cell configurations appearing in Figure S2b for $J_C^{k>k+1}$, one obtains

$$J_C^{k>k+1} \approx h\,\frac{\langle C_{1,k}E_{0,k}\rangle\langle C_{1,k}E_{1,k+1}\rangle\langle E_{0,k}E_{0,k+1}\rangle\langle E_{1,k+1}E_{0,k+1}\rangle\langle E_{1,k+1}E_{1,k+2}\rangle}{\langle C_{1,k}\rangle\langle E_{0,k}\rangle\langle E_{0,k+1}\rangle\langle E_{1,k+1}\rangle^2}$$

$$-h\,\frac{\langle C_{1,k+1}E_{0,k+1}\rangle\langle C_{1,k+1}E_{1,k}\rangle\langle E_{0,k}E_{0,k+1}\rangle\langle E_{1,k+1}E_{0,k+1}\rangle\langle E_{1,k-1}E_{1,k}\rangle}{\langle C_{1,k+1}\rangle\langle E_{0,k+1}\rangle\langle E_{0,k}\rangle\langle E_{1,k}\rangle^2}. \qquad \text{(S2.3)}$$

Using that exact relations including $\langle C_{1,k}E_{0,k}\rangle = \langle C_k\rangle$, $\langle E_{0,k}\rangle = \langle E_{int}\rangle$, $\langle E_{0.k}E_{0.k+1}\rangle = 2\langle E_{int}\rangle - 1$, etc., it follows that

$$J_C^{k>k+1} \approx h\,(2\langle E_{int}\rangle - 1)^3\langle E_{int}\rangle^{-4}\ \nabla\langle C_{k+1}\rangle. \qquad \text{(S2.4)}$$

From (S2.4), we conclude that

$$D_{tr}(2x1xL,\ R=1, \text{ pair}) = h\,(2\langle E_{int}\rangle - 1)^3/\langle E_{int}\rangle^4 = h(1 - 2\langle X_{int}\rangle)^3/(1 - \langle X_{int}\rangle)^4. \qquad \text{(S2.5)}$$

This result implies that, e.g., $D_{tr}(2x1xL,\ R=1,$ pair$) = 0.406h$ for $\langle X_{int}\rangle = 0.246$ which is significantly above $D_{tr}(\max) \approx 0.15h$ for this model with $L \geq 25$.

For the *2x2xL* cell model with $R = \sqrt{2}$, it is reasonable to implement a pair approximation which accounts for the feature that both NN and second NN pairs of cells cannot be occupied. Each of the multi-site configurations shown in Figure S2c determining the particle flux include: 3 NN CE pairs, 14 NN EE pairs, 3 second NN CE pairs, and 16 second NN EE pairs. Either the NN or second NN EE pairs produce a factor $2\langle E_{int}\rangle - 1$. Also accounting for cells shared between multiple NN and second NN pairs, we obtain

$D_{tr}(2x2xL,\ R=\sqrt{2},\ \text{pair}) = h(2\langle E_{int}\rangle - 1)^{30}/\langle E_{int}\rangle^{56} = h(1 - 2\langle X_{int}\rangle)^{30}/(1 - \langle X_{int}\rangle)^{56}.$ (S2.6)

This result implies that $D_{tr}(2x2xL,\ R=\sqrt{2},\ \text{pair}) = 0.263h$ for $\langle X_{int}\rangle = 0.136$ which is significantly above $D_{tr}(\max) \approx 0.08h$ for this model with $L \geq 25$.

S3. ANALYTIC ESTIMATES OF ADSORPTION PARAMETERS

Determination of the adsorption rate for reactants into the pore in our *2x1xL* cell model with $R = 1$ and the *2x2xL* cell model with $R = \sqrt{2}$ requires analysis of the concentration variation approaching a planar wall in a semi-infinite lattice-gas model on a simple-cubic lattice with R = 1 and $R = \sqrt{2}$, respectively. We let $\langle X_0\rangle$ denote the concentration in cells in the layer adjacent to the wall, $\langle X_{-1}\rangle$ the concentration in cells in the next layer away from the wall, etc., and $\langle X_b\rangle$ denotes the bulk concentration far from the wall. Analytic estimation of this concentration variation, and importantly of $\langle X_0\rangle$, is possible utilizing appropriate pair approximations. In this analysis, we consider the semi-infinite equilibrated fluid as having arbitrary-range exchange dynamics described by a rate f, where exchange events are consistent with range R exclusion. In equilibrium, the corresponding flux of atoms from a cell adjacent to the wall to the bulk, $J_{w\to b}$, and the reverse flux from the bulk to the wall, $J_{b\to w}$, must balance.

First, we estimate $\langle X_0\rangle$ for models with $R = 1$. The probability, P_7, of an empty cell in the bulk with all six NN cells also empty is estimated in a standard pair approximation as $P_7 \approx (1 - 2\langle X_b\rangle)^6/(1 - \langle X_b\rangle)^5$. The probability, P_6, of an empty cell against the wall with all five NN cells also empty is estimated as $P_6 \approx (1 - 2\langle X_0\rangle)^4(1 - \langle X_0\rangle - \langle X_{-1}\rangle)/(1 - \langle X_0\rangle)^4$. Then, it follows that

$$J_{w\to b} = r\langle X_0\rangle P_7 \text{ and } J_{b\to w} = r\langle X_b\rangle P_6. \quad \text{(S3.1)}$$

Assuming that $\langle X_{-1}\rangle \approx \langle X_b\rangle$, i.e., rapid decay of concentration oscillations, the equality $J_{w\to b} = J_{b\to w}$, yields $\langle X_0\rangle \approx 0.2189$ (0.1071) versus the Monte Carlo simulation values of 0.211 (0.106) for $\langle X_b\rangle = 0.20$ (0.10). The above analysis can be refined to provide additional assessment of concentration oscillations away from the wall.

For models with $R = \sqrt{2}$, we implement a pair approximation which accounts for the feature that both NN and second NN pairs of cells cannot be occupied. The probability, P_{19}, of an empty cell in the bulk with all six NN cells and all additional twelve second NN cells also empty is estimated as $P_{19} \approx (1 - 2\langle X_b\rangle)^{18}/(1 - \langle X_b\rangle)^{17}$. The probability, P_{14}, of an empty cell against the wall with all five NN cells and all additional eight second NN cells also empty is estimated as $P_{14} \approx (1 - 2\langle X_0\rangle)^8(1 - \langle X_0\rangle - \langle X_{-1}\rangle)^5/(1 - \langle X_0\rangle)^{12}$. Then, it follows that

$$J_{w\to b} = r\langle X_0\rangle P_{19} \text{ and } J_{b\to w} = r\langle X_b\rangle P_{14}. \quad \text{(S3.2)}$$

Assuming again that $\langle X_{-1}\rangle \approx \langle X_b\rangle$, the equality $J_{w\to b} = J_{b\to w}$, yields $\langle X_0\rangle \approx 0.187$ (0.081) versus the Monte Carlo simulation values of 0.123 (0.059) for $\langle X_b\rangle = 0.10$ (0.05). The above analysis can be refined to assess concentration oscillations.[1]

S4. ANALYTIC ESTIMATES OF DESORPTION PARAMETERS

To treat desorption, one needs to assess the conditional probability $Q_{5|1}$ ($Q_{9/5}$) in the *2x1xL* (*2x2xL*) cell model with $R = 1$ ($R = \sqrt{2}$). Recall that $Q_{5|1} = P_6/P_1$ denotes the conditional probability in a semi-infinite system to five empty cells NN to a specified empty cell against the wall in the semi-infinite system for $R = 1$. Here P_6 (P_1) is the probability of all 6 cells (just one cell against the wall) being empty. See Figure 3b. $Q_{9|5}$ is the conditional probability to find nine empty cells NN to a set of five empty cells against the wall for $R = \sqrt{2}$. Here P_{14} (P_5) is the probability of all 14 cells (just 5 cells against the wall) being empty. See Figure 4b.

For the *1x1xL* cell model with $R = 1$, a standard pair approximation leads to the estimate $P_6 \approx \langle E_{0,0,-1}E_{0,0,0}\rangle\langle E_{0,0,0}E_{1,0,0}\rangle\langle E_{0,0,0}E_{0,1,0}\rangle\langle E_{0,0,0}E_{-1,0,0}\rangle\langle E_{0,0,0}E_{0,-1,0}\rangle/\langle E_0\rangle^4$. Since $\langle E_{0,0,-1}E_{0,0,0}\rangle = 1 - \langle X_0\rangle - \langle X_{-1}\rangle$, $\langle E_{0,0,0}E_{1,0,0}\rangle = 1 - 2\langle X_0\rangle$, etc., and $\langle E_0\rangle = 1 - \langle X_0\rangle = P_1$, it follows that

$$Q_{5|1}(pair) = P_6/P_1 = (1 - \langle X_0\rangle - \langle X_{-1}\rangle)(1 - 2\langle X_0\rangle)^4/(1 - \langle X_0\rangle)^5. \quad \text{(S4.1)}$$

For $\langle X_b\rangle = 0.2$, we conclude that $Q_{5|1}(pair) = 0.237$ (0.213) just using $\langle X_0\rangle \approx \langle X_{-1}\rangle \approx \langle X_b\rangle = 0.2$ (using simulation values of $\langle X_0\rangle = 0.212$ and $\langle X_{-1}\rangle = 0.199$). These compare with the simulation value of $Q_{5|1} = 0.279$ for $\langle X_b\rangle = 0.2$. For $\langle X_b\rangle = 0.1$, we conclude that $Q_{5|1}(pair) = 0.555$ just using $\langle X_0\rangle \approx \langle X_{-1}\rangle \approx \langle X_b\rangle = 0.1$, compared to the simulation value of $Q_{5|1} = 0.547$.

For the *2x2xL* cell model with $R = \sqrt{2}$, we implement a pair approximation which accounts for the feature that both NN and second NN pairs of cells cannot be occupied. P_{14} is factorized into 4 NN pairs and 4 second NN pairs in layer $k = -1$, 12 NN pairs and 8 second NN pairs in layer $k = 0$, and 5 NN pairs and 16 second NN pairs with one empty cell in layer $k = 0$ and the other in layer $k = -1$. Likewise, P_5 factorizes into 4 NN pairs and 4 second NN pairs in layer $k = 0$. One concludes that

$$Q_{9|5}(pair) = P_{14}/P_5$$

$$= (1 - \langle X_0\rangle - \langle X_{-1}\rangle)^{21}(1 - 2\langle X_{-1}\rangle)^8\,(1 - 2\langle X_0\rangle)^{12}/[(1 - \langle X_{-1}\rangle)^{32}(1 - \langle X_0\rangle)^{41}]. \quad \text{(S4.2)}$$

For $\langle X_b\rangle = 0.1$ (0.05), we conclude that $Q_{5|1}(pair) = 0.233$ (0.562) just using $\langle X_0\rangle \approx \langle X_{-1}\rangle \approx \langle X_b\rangle = 0.1$ (0.05), compared to the simulation value of $Q_{5|1} = 0.194$ (0.533).

S5. ADDITIONAL ANALYSIS OF TRACER EXCHANGE

Here, we provide a more complete presentation of results than in Sec.4.3 for TE where the pore is initially populated by B and the exterior reservoir by A (and the total concentration is equilibrated). Figure S5.1 shows the evolution of concentration profiles both for A entering the pore and for B exiting the pore. In Figure S5.2, we show the corresponding tracer exchange curve, $\gamma(t)$, versus t, where $\gamma(t)$ simply gives the fraction of particles inside the pore which are of type A at time t.

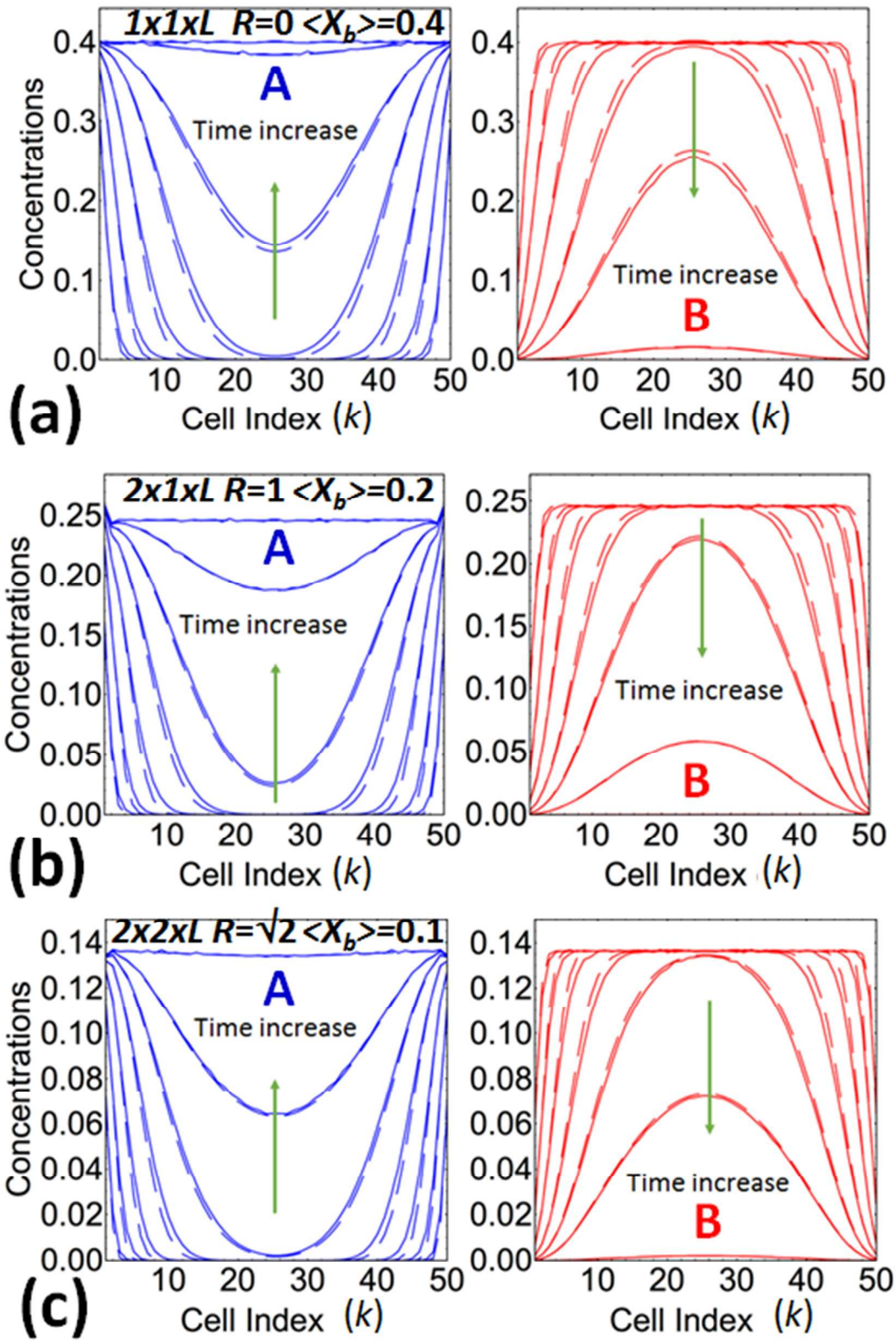

Figure S5.1. Profile evolution for tracer exchange for the three models. Time: 0, 5, 5^2,…, 5^7. Solid curves: KMC simulation. Dashed curves: generalized hydrodynamic theory.

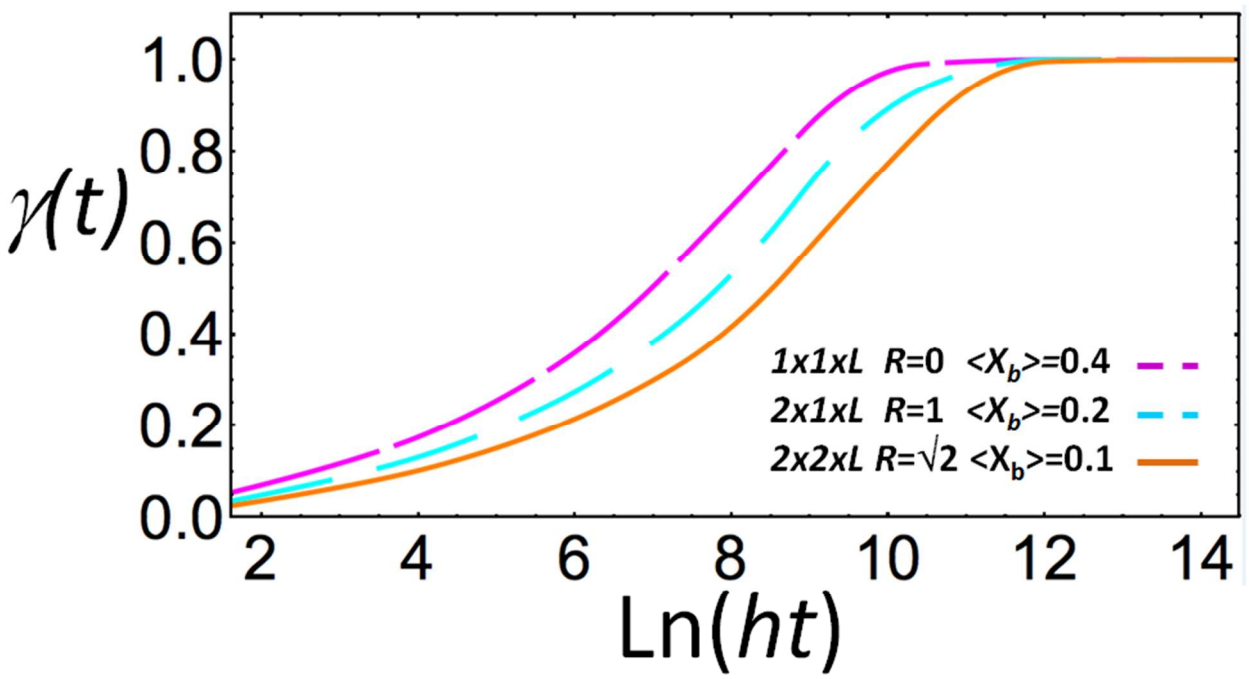

Figure S5.2. Simulated tracer exchange curves for the three models illustrated in Figure S5.1.

REFERENCES

(1) Garcia, A.; Evans, J.W. Catalytic Conversion in Nanoporous Materials: Concentration Oscillations and Spatial Correlations due to Inhibited Transport and Intermolecular Interactions. *J. Chem. Phys.* **2016**, *145*, 174705.